

PAPER • OPEN ACCESS

Model Establishment and Parameter Identification of Remotely Operated Vehicle (ROV)

To cite this article: Yelei Zhang *et al* 2024 *J. Phys.: Conf. Ser.* **2785** 012107

View the [article online](#) for updates and enhancements.

You may also like

- [Target recognition using rotating ultrasonic sensor for an amphibious ROV](#)
Jiangfei Yang, Boshen Liu, Fei Ma et al.
- [Proposed Mathematical Modeling of Small Remotely Operated Vehicle \(ROV\) Movement](#)
Iis Hamsir Ayub Wahab, Rintania Elliyati Nuryaningsih and Achmad Pradjudin Sardju
- [The preliminary of Design and Movement of Remotely Operated Vehicle \(ROV\)](#)
S Manullang, A Pusaka and A Setiawan

PRIME
PACIFIC RIM MEETING
ON ELECTROCHEMICAL
AND SOLID STATE SCIENCE

HONOLULU, HI
October 6-11, 2024

Joint International Meeting of
The Electrochemical Society of Japan (ECS)
The Korean Electrochemical Society (KECS)
The Electrochemical Society (ECS)

Early Registration Deadline:
September 3, 2024

MAKE YOUR PLANS NOW!

Model Establishment and Parameter Identification of Remotely Operated Vehicle (ROV)

Yelei Zhang ¹, Baoji Yin ^{1,*}, Huifeng Jiao ², Jian Zhang ¹, and Fei Yan ¹

¹ School of Mechanical Engineering, Jiangsu University of Science and Technology, Zhenjiang 212003, China

² State Key Laboratory of Deep-Sea Manned Vehicles, China Ship Scientific Research Center, Wuxi 214082, China

*E-mail: yinbaoji@just.edu.cn

Abstract: To study the dynamic characteristics of remotely operated vehicle (ROV) underwater motion, a transformation matrix between the carrier coordinate system and the inertial coordinate system was established, and the rigid body dynamics model of the ROV was derived by using the Newton-Euler equation. According to the results of the ROV experimental prototype in this article, the dynamic model is simplified based on the force, motion characteristics, and structural characteristics. In the pool experiment, based on the propeller dynamic model, the least squares method was used to identify the parameters of the heading and vertical dynamic models, and through the experimental results under step control signals of different amplitudes, they were compared with the models under the same control signal. The output is subjected to error analysis. The experimental results show that the error between the theoretical value and the experimental value is small, verifying the accuracy of the ROV dynamics model established in this article.

1. Introduction

With the development of the marine industry, remotely operated vehicle (ROV) is widely used in lakes, reservoirs, and ports to engage in maintenance, exploration, etc. [1]. Since the underwater environment is difficult to predict, the ROV must be simulated through experiments and its motion patterns must be analyzed first to ensure the autonomy and safety of the ROV. Therefore, it is necessary to first establish a model for the ROV and identify its corresponding hydrodynamic parameters.

Regarding how to identify the corresponding parameters of ROV, Yu adopted the empirical formula method [2], but this method cannot accurately obtain the relevant hydrodynamic coefficients. To this end, this article adopts an experimental method to determine the hydrodynamic coefficient by measuring the actual movement speed of the ROV in the water based on the relationship between the external force and the movement speed of the ROV. Since ROV has six degrees of freedom when moving in water and behaves as a high-intensity nonlinear coupling system, this article establishes and simplifies the ROV kinematics and dynamics model. In addition, to reduce the complexity of multi-degree-of-freedom coupled motion, this article decomposes the dynamic model into single-degree-of-freedom motion, so that the influence of the propeller on the underwater motion of the ROV in this article can be intuitively described.



2. Structural design and kinematic model of ROV

2.1 ROV structural design

The ROV designed in this article can be divided into three parts at the mechanical structure level: streamlined shell, aluminum profile frame, and electronic cabin. The electronic cabin, thrusters, and sensors are installed on the frame respectively, and the thrusters and sensors are integrated with the electronic cabin through watertight connectors. The overall structure of the ROV is shown in Figure 1.

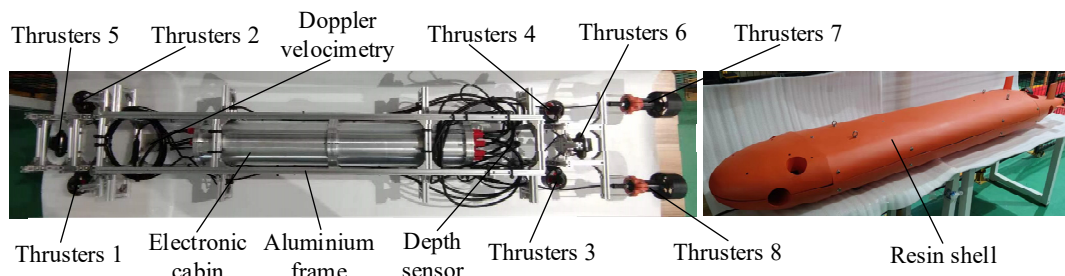


Figure 1. Physical diagram of the overall structure of ROV.

2.2 Kinematic model of ROV

Referring to the terminology bulletin of the International Tank Conference (ITTC) and the Society of Naval Architecture and Marine Engineering (SNAME) [3], the ROV inertial coordinate system $E-\xi\eta\zeta$ and the carrier coordinate system $O-xyz$ are established, as shown in Figure 2. The specific motion parameters and mechanics are shown in Table 1.

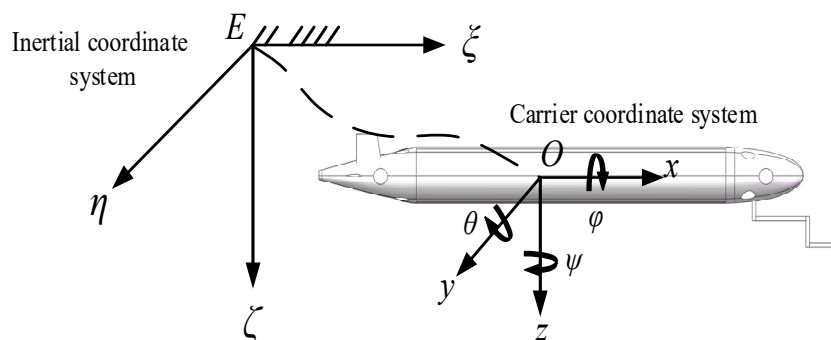


Figure 2. Schematic diagram of the ROV coordinate system.

Table 1. ROV motion parameters and mechanical parameters.

Name	Position and angle	Linear velocity and angular velocity	Forces and moments
Vertical movement	x	u	X
Lateral movement	y	v	Y
Vertical movement	z	w	Z
Rolling motion	φ	p	K
Pitching motion	θ	q	M
Heading motion	ψ	r	N

Because the state variables such as linear velocity and angular velocity of ROV are measured based on sensors in the carrier coordinate system, Newton's law and Euler's equation are only established in the inertial coordinate system. Therefore, it is necessary to establish a conversion between the carrier coordinate system and the inertial coordinate system equation.

$$\mathbf{J}_v = \begin{bmatrix} \cos \psi \cos \theta & \cos \psi \sin \theta \sin \varphi - \sin \psi \cos \varphi & \cos \psi \sin \theta \cos \varphi + \sin \psi \sin \varphi \\ \sin \psi \cos \theta & \sin \psi \sin \theta \sin \varphi + \cos \psi \cos \varphi & \sin \psi \sin \theta \cos \varphi - \cos \psi \sin \varphi \\ -\sin \theta & \cos \theta \sin \varphi & \cos \theta \cos \varphi \end{bmatrix} \quad (1)$$

where \mathbf{J}_v is the transformation matrix for displacement and linear velocity from the carrier coordinate system to the inertial coordinate system.

$$\mathbf{J}_w = \begin{bmatrix} 1 & \sin \varphi \tan \theta & \cos \varphi \tan \theta \\ 0 & \cos \varphi & -\sin \varphi \\ 0 & \sin \varphi \sec \theta & \cos \varphi \sec \theta \end{bmatrix} \quad (2)$$

where \mathbf{J}_w is the transformation matrix for angle and angular velocity from the carrier coordinate system to the inertial coordinate system.

The kinematic model of the ROV converted from the carrier coordinate system to the inertial coordinate system is:

$$\begin{bmatrix} \dot{\eta}_1 \\ \dot{\eta}_2 \end{bmatrix} = \begin{bmatrix} \mathbf{J}_v & \mathbf{O}_{3 \times 3} \\ \mathbf{O}_{3 \times 3} & \mathbf{J}_w \end{bmatrix} \begin{bmatrix} \mathbf{v}_1 \\ \mathbf{v}_2 \end{bmatrix} \quad (3)$$

where $\eta_1 = [\xi, \dot{\eta}, \zeta]^T$, $\eta_2 = [\phi, \dot{\theta}, \dot{\psi}]^T$, $\mathbf{v}_1 = [u, v, w]^T$, and $\mathbf{v}_2 = [p, q, r]^T$.

3. Establishment and simplification of dynamic model of ROV

To reduce the complexity of the model and facilitate subsequent research, the ROV designed in this article has the following characteristics:

(1) The center of gravity of the ROV designed in this article coincides with the origin of the motion coordinate system. Its shape is flat and can be approximately regarded as symmetrical about xOy, xOz, and yOz and the ROV has a low speed in the water.

(2) The ROV has been manually trimmed before moving. By adding buoyancy materials inside the fuselage, the roll and pitch angles of the ROV are 0. The center of buoyancy of the ROV is slightly higher than the center of gravity, and the buoyancy and gravity are approximately equal.

According to the above characteristics, the ROV dynamics model is simplified as:

$$\mathbf{M} \dot{\mathbf{v}} + \mathbf{D}(\mathbf{v}) \mathbf{v} = \boldsymbol{\tau} \quad (4)$$

where \mathbf{M} is the mass and inertia matrix, $\mathbf{D}(\mathbf{v})$ is the fluid resistance matrix, and $\boldsymbol{\tau}$ is the propeller thrust and moment matrix. \mathbf{M} and $\mathbf{D}(\mathbf{v})$ can be expressed as:

$$\mathbf{M} = \text{diag} \{ m - X_{\ddot{u}}, m - Y_{\ddot{v}}, m - Z_{\ddot{w}}, 0, I_y - M_{\dot{q}}, I_z - N_{\dot{r}} \} \quad (5)$$

$$\mathbf{D}(\mathbf{v}) = \text{diag} \{ X_u + X_{u|u}|u|, Y_v + Y_{v|v}|v|, Z_w + Z_{w|w}|w|, 0, M_q + M_{q|q}|q|, N_r + N_{r|r}|r| \} \quad (6)$$

The thrust generated by the thruster is the main power source of the ROV. The ROV designed in this article is equipped with a total of eight thrusters, including two thrusters in the longitudinal and transverse directions, and four thrusters in the vertical axis. The location is shown in Figure 3.

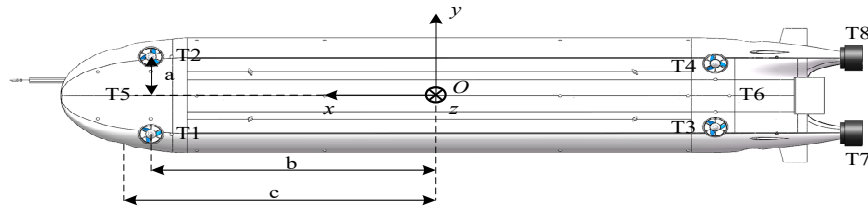


Figure 3. ROV thruster layout diagram.

The six-degree-of-freedom thrust and moment equations of the ROV thruster in the carrier coordinate system can be expressed as:

$$\boldsymbol{\tau} = \begin{bmatrix} X_T \\ Y_T \\ Z_T \\ K_T \\ M_T \\ N_T \end{bmatrix} = \begin{bmatrix} T_7 + T_8 \\ (T_5 + T_6)\varepsilon \\ T_1 + T_2 + T_3 + T_4 \\ (-T_1 + T_2 - T_3 + T_4)a \\ (-T_1 - T_2 + T_3 + T_4)b \\ (T_5 - T_6)\varepsilon c \end{bmatrix} \quad (7)$$

where $T_1 \sim T_8$ is the thrust generated by the eight thrusters of the ROV; ε is the thrust loss coefficient of the lateral thrusters, which is taken to be 70%; a is the distance from the vertical thrusters to the x -axis, which is 0.147 m; b is the distance from the vertical thrusters to the y -axis and the distance is 0.827 m; c it is the distance from the lateral thruster to the z -axis, which is 0.921 mm.

Further, the simplified dynamic model is decoupled into a single-degree-of-freedom dynamic model.

$$m_\xi \ddot{\xi} + d_\xi \dot{\xi} + d_{\xi|\xi} |\dot{\xi}| \xi = \tau_\xi \quad (8)$$

where ξ is the direction of the degree of freedom, m_ξ is the inertia coefficient, d_ξ is the primary resistance coefficient, $d_{\xi|\xi}$ is the secondary resistance coefficient, and τ_ξ is the component of the propeller thrust or moment in the direction of the degree of ξ freedom.

4. Identification of dynamic model parameters of ROV

4.1 Overview of least squares method

The least squares method is a mathematical method for fitting data and estimating parameters [4]. Its goal is to find a set of parameters that minimize the sum of squared residuals between the model's predicted values and the actual observed values.

Therefore, in Formula (8), the following relationship is established through the least squares method.

$$\underbrace{\begin{bmatrix} \tau_{\xi,1} \\ \vdots \\ \tau_{\xi,k} \\ \vdots \\ \tau_{\xi,n} \end{bmatrix}}_y = \underbrace{\begin{bmatrix} \dot{v}_{\xi,1} & v_{\xi,1} & v_{\xi,1} | v_{\xi,1} \\ \vdots & \vdots & \vdots \\ \dot{v}_{\xi,k} & v_{\xi,k} & v_{\xi,k} | v_{\xi,k} \\ \vdots & \vdots & \vdots \\ \dot{v}_{\xi,n} & v_{\xi,n} & v_{\xi,n} | v_{\xi,n} \end{bmatrix}}_H \underbrace{\begin{bmatrix} m_\xi \\ d_\xi \\ d_{\xi|\xi} \\ \theta \end{bmatrix}}_\theta \quad (9)$$

The least squares estimate that can be obtained according to the above formula is:

$$\hat{\theta}_{LS} = (H^T H)^{-1} H^T y \quad (10)$$

4.2 Dynamic model of thruster

Based on the propeller dynamics model proposed by Fossen, due to the low underwater navigation speed of the ROV in this article, according to Avila et al. [5], this article does not consider the motor characteristics of the propeller, and the rotation speed of the propeller can be obtained. There is an approximate binomial relationship with the control voltage. The dynamic model to establish the controllable voltage and thrust of the thruster is:

$$T = aV^2 + bV + c \quad (11)$$

where T is the propeller thrust; a, b, and c are constants to be estimated.

As shown in Figure 4 (a), with the help of the thruster test system device, the data of the thrust generated by the thruster and its control voltage during forward and reverse rotation were measured. During the experiment, the control voltage was slowly increased from -2.4 V to 2.4 V with a step increment of 0.2 V, and the control voltage and corresponding thrust value of the thruster were obtained. Considering that the situation of the propeller in forward and reverse rotation is not consistent, the measured thrust and control voltage are fitted piecewise through the MATLAB least squares fitting program. The thruster fitting curve is shown in Figure 4 (b).

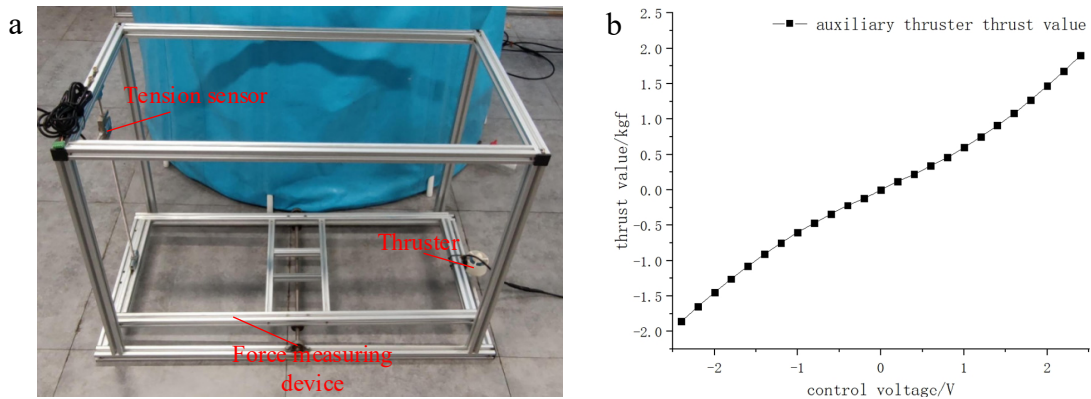


Figure 4. Thruster force measuring device and thrust curve diagram.

The expressions for the control voltage and thrust of the thruster can be obtained as follows:

$$\begin{aligned} T_{\text{reverse}} &= -0.132V^2 + 0.407V - 0.005 \\ T_{\text{forward}} &= -0.064V^2 + 0.932V + 0.032 \end{aligned} \quad (12)$$

4.3 Parameter identification experiment of the dynamic model

4.3.1 Identification of heading dynamics model parameters. According to the Formula (8), the ROV heading dynamics model in the carrier coordinate system is:

$$m_r \dot{r} + d_r r + d_{r|r} r |r| = \tau_r \quad (13)$$

We set the control voltage signal of the thruster to a triangular wave signal with an amplitude of -2.0~2.0 V and a frequency of 1/40 Hz, and collect the ROV's heading angular velocity and angular acceleration through the HWT950 inclinometer. The experimental results are shown in Figure 5.

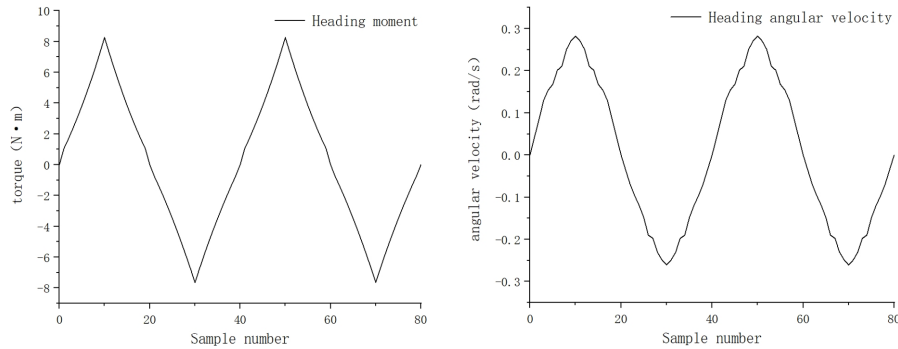


Figure 5. ROV heading test of 1/40 Hz triangular wave control voltage signal

According to the measured data in Figure 5, the heading torque value generated by the corresponding control voltage and the measured heading angular velocity and angular acceleration are brought into Formula (13), and the least squares method can be obtained:

$$\begin{aligned} m_r &= 7.396 \text{ kg} \cdot \text{m}^2 \\ d_r &= 19.901 \text{ N} \cdot \text{m} (\text{rad} / \text{s}) \\ d_{r|r|} &= 46.460 \text{ N} \cdot \text{m} (\text{rad} / \text{s})^2 \end{aligned} \quad (14)$$

Therefore, the heading dynamics model of ROV is:

$$7.396\dot{r} + 19.901r + 46.460r|r| = \tau_r \quad (15)$$

4.3.2 Vertical dynamics model parameter identification. According to the Formula (8), the ROV vertical dynamics model in the carrier coordinate system is:

$$m_w \dot{w} + d_w w + d_{w|w|} w|w| = \tau_w \quad (16)$$

We set the control voltage signal of the thruster to a triangular wave signal with an amplitude of -2.0~2.0 V and a frequency of 1/40 Hz, and use the PCM260 depth gauge to collect the vertical depth of the ROV. At the same time, we differentiate the depth with time to obtain the vertical velocity and differentiate the vertical velocity with time to obtain the vertical acceleration. The experimental results are shown in Figure 6.

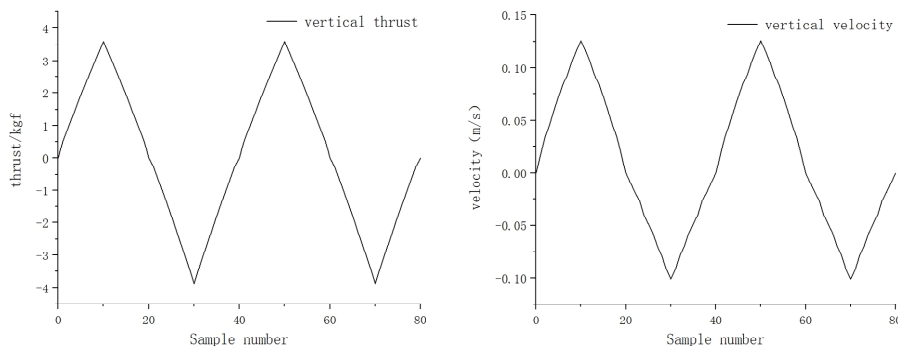


Figure 6. ROV vertical test of 1/40 Hz triangular wave control voltage signal .

According to the measured data in Figure 6, the vertical thrust generated by the corresponding control voltage and the vertical velocity and vertical acceleration obtained by measurement and calculation are brought into Formula (16). Through the least squares method, it can be obtained:

$$\begin{aligned}
 m_w &= -4.206 \text{ kg} \\
 d_w &= 24.920 \text{ N} \cdot \text{m} (\text{m/s}) \\
 d_{w|w} &= 34.304 \text{ N} \cdot \text{m} (\text{m/s})^2
 \end{aligned}
 \tag{17}$$

Therefore, the vertical dynamics model of ROV is:

$$-4.206\dot{w} + 24.920w - 34.304w|w| = \tau_w
 \tag{18}$$

To verify the accuracy of the single degree of freedom dynamic model obtained by the above parameter identification experiment, it is necessary to apply step control voltage signals of different amplitudes to the ROV thruster. First, the fourth-order Runge-Kutta method is used to solve the problems separately. The differential equation of the heading dynamic model and the differential equation of the vertical dynamic model are used to obtain the theoretical value of the heading angular velocity and vertical velocity respectively; Then, the measured values of the ROV heading angular velocity and the vertical velocity are respectively collected through experiments; Finally, the identification effect is verified by comparative analysis of heading angular velocity error and vertical velocity error. The single-degree-of-freedom experimental records drawn are shown in Figures 7 and 8:

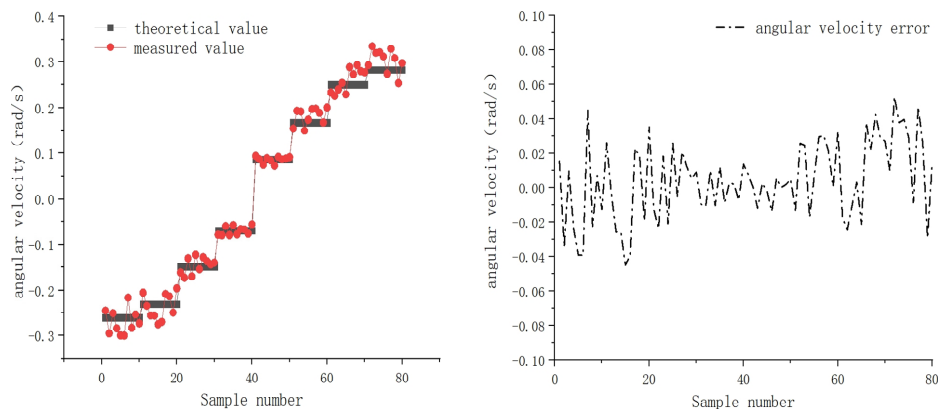


Figure 7. Step control of voltage, heading, angular velocity, and error.

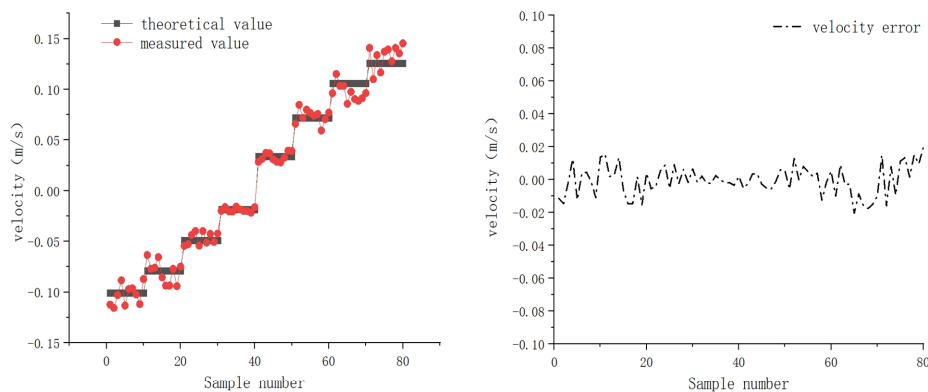


Figure 8. Step control of voltage, vertical velocity, and error.

According to Figures 7 and 8, the heading angular velocity error and vertical velocity error of the above two sets of verification experiments were analyzed, and the absolute error, relative error, and error label difference of the two sets of experiments were calculated respectively. The results are shown in Table 2.

Table 2. Analysis results of angular velocity and velocity error .

Single degree of freedom name	Absolute error range	Maximum relative error	Standard deviation
Heading motion	-0.0447~0.0528 rad/s	24.69%	0.0228 rad/s
Vertical movement	-0.0204~0.0194 m/s	24.28%	0.0091 m/s

5. Conclusions

This paper mainly studies the offline identification of the ROV heading dynamic model using the least squares method based on the identification premise of the ROV propeller dynamic model in the pool experiment. We input different thruster step control voltage signals to obtain the actual speed, and use Runge-Kutta to output the theoretical speed of the model. The absolute error of the heading angular velocity is approximately stable between -0.0447 rad/s~0.0528 rad/s, the maximum relative error is 24.69%, and the standard deviation of the angular velocity error is 0.0228 rad/s. The absolute error of the vertical movement velocity is approximately stable at between -0.0204 m/s and 0.0194 m/s, the maximum relative error is 24.28%, and the standard deviation of the speed error is 0.0091 m/s. By comparing the error between the actual speed and the model output, the correctness of the ROV dynamics model established in this article is verified.

Acknowledgments

This research received funding from the National Natural Science Foundation of China [Grant number: 52201365], and the Postgraduate Research & Practice Innovation Program of Jiangsu Province [Grant number: SJCX22_1925].

References

- [1] Tomoya I., Tokihiro K., Hisataka M., et al. (2009). Crawler System for Deep Sea ROVs. *Marine Technology Society Journal*, 43 (5): 97-104.
- [2] Yu H. (2003). Research on identification and control technology of open-frame underwater vehicles. Harbin Engineering University.
- [3] Zhu D., Yuan Y., and Deng Z. (2015). Quantum particle swarm optimization algorithm for parameter identification of the underwater vehicle. *Control Engineering*, (1): 531-537.
- [4] Huang Y., Fang Y., Liu P., et al. (2021). A RTCP automatic measurement cycle based on the least square method. *Manufacturing Technology and Machine Tools*, (1): 114-118.
- [5] Avila J., Adamowski J. C., Maruyama N., et al. (2012). Modeling and Identification of an Open-Frame Underwater Vehicle. *Journal of Intelligent and Robotic Systems*, 66 (1): 37-56.